Chinese Chemical Letters 35 (2024) 109890

Contents lists available at ScienceDirect

Chinese Chemical Letters

journal homepage: www.elsevier.com/locate/cclet

# Development of Mg-Al LDH and LDO as novel protective materials for deacidification of paper-based relics

Sinong Wang[a,d,1,*], Shanshan Jin[a,1], Xue Yang[b], Yanyan Huang[a], Peng Liu[a,d], Yi Tang[b,*], Yuliang Yang[a,c]

[a] *Institute for Preservation and Conservation of Chinese Ancient Books, Fudan University Library, Fudan University, Shanghai 200433, China*

[b] *Department of Chemistry, Shanghai Key Laboratory of Molecular Catalysis and Innovative Materials, Collaborative Innovation Centre of Chemistry for Energy Materials, Fudan University, Shanghai 200433, China*

[c] *State Key Laboratory of Molecular Engineering of Polymers, Department of Macromolecular Science, Fudan University, Shanghai 200433, China*

[d] *Key Laboratory of Pulp and Paper Science & Technology of Ministry of Education, Qilu University of Technology (Shandong Academy of Sciences), Ji'nan 250353, China*

ARTICLE INFO

*Article history:*
Received 24 October 2023
Revised 17 March 2024
Accepted 15 April 2024
Available online 18 June 2024

*Keywords:*
Layered double hydroxide
Layered double oxide
Structural memory effect
Paper protection
Deacidification

## ABSTRACT

Acidification of paper-based relics is a common problem, leading to their degradation and eventual loss. Paper deacidification is highly dependent on a limited variety of alkaline materials, and the development of new materials that are safe, efficient and easy-to-prepare is highly demanded to ensure a high level of safety and effective protection of paper-based relic. This study proposes the introduction of layered double hydroxide (LDH) and its calcined product, mixed metal oxide (layered double oxide (LDO)), as innovative protective materials for the deacidification of paper with varying levels of acidity. The results demonstrate that treatment with Mg-Al LDH/LDO can effectively modify the pH of acidic paper (*e.g.*, pH $\sim$ 4.0–6.4) to a neutral or weakly basic state, maintaining this desirable pH range even under long-term accelerated aging condition. Remarkably, LDH proves to be well-suited for the protection of slightly acidified paper (*e.g.*, pH $>$ 5.5), while LDO serves as an especially option for the deacidification of severely acidified paper (*e.g.*, pH $\leq$ 5.5). During aqueous deacidification, due to the memory effect of the LDH-based materials, LDO is converted to rehydrated LDH, which creates a mild and appropriate alkaline retention in the paper, avoiding damage caused by strong alkalinity such as cellulose degradation and pigment fading during subsequent long-term natural preservation of the paper. Furthermore, Mg-Al LDH/LDO materials also exhibit flame-retardant and bacteriostatic properties. This opens up opportunities for the safe, efficient and multifunctional protection of acidified paper-based relics.

Paper has been an essential part of human civilization as a writing/printing medium for recording information and inheriting culture. However, it is prone to aging degradation and even destroy over time [1,2], and thus great efforts should be made for the protection of paper and paper-based cultural relics ensuring their transfer to future generations. China's 14th Five-Year Plan has explicitly called for the strengthening of the protection, research, and utilization of cultural relics, creating new opportunities for the application of science and technology in the preservation of paper-based cultural relics. It is well known that acid-catalyzed hydrolysis of cellulose macromolecules is the most fatal cause of paper degradation, in which the cleavage of $\beta-1,4$-glycosidic bond leads to depolymerization of cellulose chains and consequently shortens the longevity of paper [3–5]. Liquid-phase deacidification, considered one of the most effective and widely applied methods, involves immersing paper in deacidifying agent to neutralize existing free acids and deposit alkaline substances in the fibers for the newly generated acids during subsequent aging [6]. Until now, several kinds of alkaline materials have been used for paper deacidification, such as amines, alkaline compounds of calcium and magnesium, *etc.*, based on the principle of minimum intervention required for paper deacidification [7–9]. In addition, composite materials have been applied for multifunctional protection of paper-based materials, *e.g.*, simultaneous use of calcium hydroxide ($Ca(OH)_2$) and methyl cellulose for mass

---

[*] Corresponding authors.
*E-mail addresses:* wangsn@fudan.edu.cn (S. Wang), yitang@fudan.edu.cn (Y. Tang).

[1] These authors contributed equally to this work.

https://doi.org/10.1016/j.cclet.2024.109890
1001-8417/

deacidification and strengthening of newspaper [10], magnesium oxide/$Ca(OH)_2$/epoxypropyl trimethyl ammonium chloride composites for deacidification, strengthening and antifungal of book [11], layer-by-layer assembly of chitosan and montmorillonite for fire retardant on Xuan paper [12]. Indeed, developing safe, efficient, and versatile deacidifying materials is crucial. Moreover, it should be noted that the inappropriate alkalinity of deacidifying materials may have adverse effects on paper and writings/drawings, such as secondary degradation pathways (*e.g.*, alkaline degradation [13] and autoxidation [14], photosensitive reaction [15]) and discoloration of pigments. Accordingly, there is a strong desire to discover deacidifying materials with suitable and adjustable alkalinity, along with large surface area, economic cost and non-toxicity for paper multifunctional protection to long-term safety and efficiency.

Layered double hydroxide (LDH) represents a class of ionic lamellar materials, with a general formula of $[M^{2+}{}_{1\text{-}y}M^{3+}{}_{y}(OH)_2]^{y+}(A^{n-})_{y/n}{\cdot}zH_2O)$, where $M^{2+}$, $M^{3+}$, and $A^{n-}$ denote divalent cations, trivalent cations and anions, respectively [16]. Their unique chemical structure and properties, such as tunability of composition and structure, good thermal stability, resistance to pH variation and flame-retardant properties, have enabled their widespread applications as catalysts [17], flame retardants [18], drug carriers [19], and adsorbents [20]. In addition, LDH has a similar basicity to its constituent divalent metal hydroxide. After calcination in air, LDH transforms into mixed metal oxide, known as layered double oxide (LDO), which offers additional basic sites. Remarkably, LDO can subsequently be rehydrated, restoring its structure partially to LDH with an ordered layered structure, a phenomenon referred to as the "memory effect" [21]. This characteristic not only modifies the structure of LDH-based material but also imparts it with adjustable alkalinity. Furthermore, simple synthetic methods are available to regulate the alkalinity of such layered materials by adjusting their thickness and composition *via* surfactant-assistance [22,23]. All of these features make LDH-based material a promising candidate for the safe deacidification and multi-protection (*e.g.*, flame retardant) of paper-based relics.

Recently, Jurišová reported that changing the alkalinity of hydrotalcites by varying the Mg:Al ratio and dispersing them in ternary solutions (perfluoroheptane/isopropanol/water) were used for paper deacidification, and the results showed that the pH of acidic paper (pH~4) could be increased to the range of 4.6–7 [24]. Based on the memory effect of LDH-based materials, herein, we report a novel application of Mg-Al LDH and Mg-Al LDO for deacidification of paper with varying levels of acidity (Scheme 1). Mg-Al LDH was synthesized by simple hydrothermal method, and then calcined at 500 °C in air to obtain Mg-Al LDO. Handmade bamboo paper (BP) with a wide range of acidity and dry-heat accelerated aging test were used to evaluate the effectiveness of liquid-phase deacidification of Mg-Al LDH and LDO. The results indicate that LDH is suitable for the protection of mildly acidified paper (*e.g.*, pH > 5.5), whereas LDO is effective for deacidifying severely acidified paper (*e.g.*, pH ≤ 5.5), and that during aqueous deacidification, LDO creates a mild and appropriate alkaline retention in the paper through its conversion to rehydrated LDH due to the memory effect. Moreover, Mg-Al LDH/LDO also demonstrates good flame retardancy, bacterial resistance and protection against color fading.

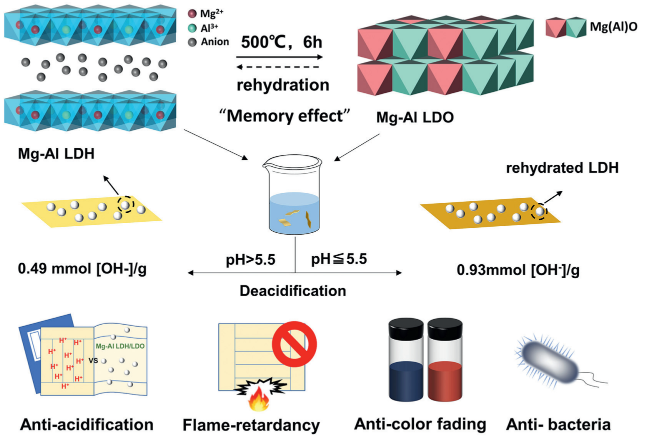

**Scheme 1.** Schematic illustration of Mg-Al LDH and Mg-Al LDO for paper protection.

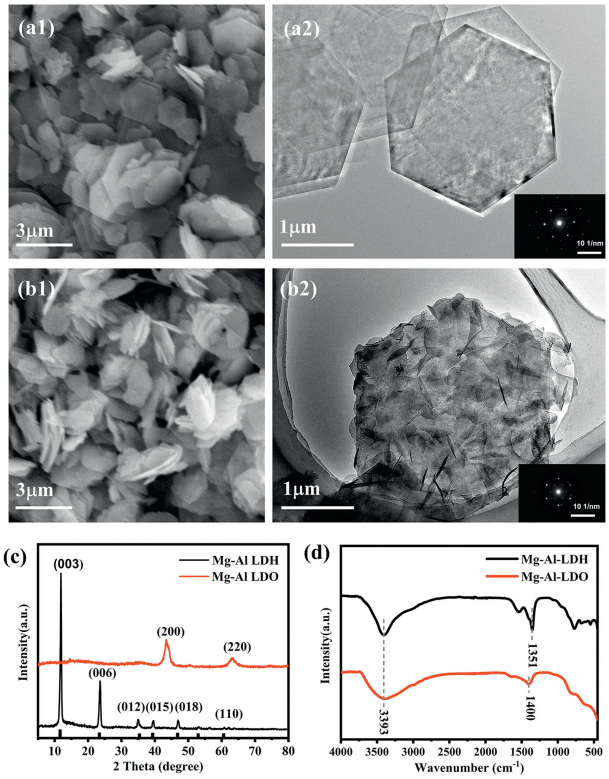

**Fig. 1.** ($a_1$, $a_2$) SEM and TEM images of Mg-Al LDH. ($b_1$, $b_2$) SEM and TEM images of Mg-Al LDO. Inset of ($a_2$, $b_2$) SAED patterns of the corresponding materials. (c) XRD patterns and (d) FT-IR spectra of Mg-Al LDH and Mg-Al LDO.

The scanning electron microscopy (SEM) and transmission electron microscopy (TEM) images (Figs. 1$a_1$ and $a_2$) show the hexagonal shape with several micrometers in size of the as-synthesized Mg-Al LDH nanoflakes. Inset in Fig. 1$a_2$ is the corresponding selected area electron diffraction (SAED) pattern where the hexagonally arranged spots can be indexed to the 110 crystalline plane family of Mg-Al LDH. Strong X-ray diffraction (XRD, Fig. 1c) peaks corresponding to (003) and (006) faces demonstrate the excellent layered feature and fine crystallinity of Mg-Al LDH (JCPDS No. 70–2151) [25]. A series of (012), (015), (018) and (110) peaks prove that Mg-Al LDH has hexagonal lattice with rhombohedral 3R symmetry due to $CO_3{}^{2-}$ intercalation [26]. The present of $CO_3{}^{2-}$ in the interlayer is further confirmed by the Fourier transform infrared spectroscopy (FT-IR) spectrum (Fig. 1d), where the absorption peak at 1400 $cm^{-1}$ is attributed to the interlayer $CO_3{}^{2-}$ anions. After calcination at 500 °C, the hydrotalcite Mg-Al LDH structure undergoes transformation through the elimination of carbonate anions and water molecules, ultimately leading to the formation of Mg-Al LDO [27]. XRD analysis (Fig. 1c) reveals the appearance of two broad diffraction peaks at (200) and (220), which can be attributed to MgO in Mg-Al LDO. Meanwhile, other peaks related to $Al_2O_3$ disappear due to the transformation of Al into the lattice of MgO

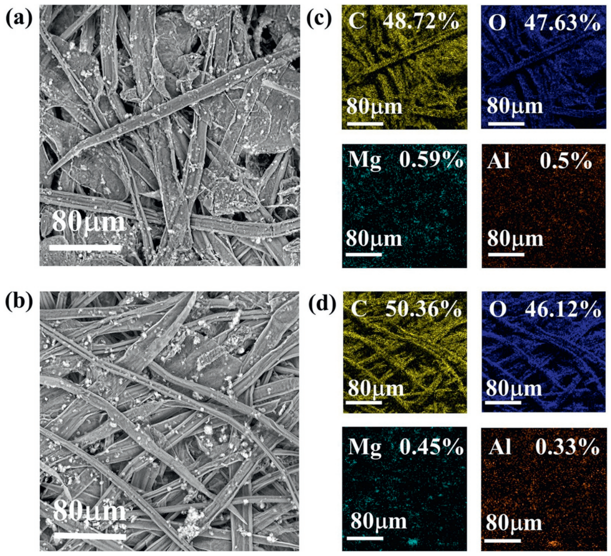

**Fig. 2.** SEM images of (a) Mg-Al LDH-BP, and (b) Mg-Al LDO-BP, EDS mapping of (c) Mg-Al LDH-BP and (d) Mg-Al LDO-BP.

during the calcination processes [28]. FT-IR analysis (Fig. 1d) further illustrates these findings, revealing shifts in the bands corresponding to the lattice vibrations of Mg-O and Al-O in Mg-Al LDO towards lower wavenumbers. After calcination, the LDO retains the good hexagonal shape with dimensions in several micrometers, but its structure becomes loose (Figs. $1b_1$ and $b_2$). Meanwhile, the results calculated from the $N_2$ sorption isotherm (Fig. S1 in Supporting information) show that the Brunauer-Emmett-Teller (BET) surface area of Mg-Al LDO is measured to be 283.2 $m^2/g$, which is significantly larger than that of Mg-Al LDH (47.2 $m^2/g$). Moreover, Mg-Al LDO exhibits an obvious pore structure with a pore size of 1.3 nm resulting from the structural destruction inside the hydrotalcite Mg-Al LDH during calcination in air. ICP-AES analysis shows similar values of the molar ratio of $Mg^{2+}/Al^{3+}$ in Mg-Al LDH and LDO (Table S1 in Supporting information).

The liquid-phase method was employed for the deacidification of paper, in which acidified bamboo paper (BP) was immersed in 0.5 wt% Mg-Al LDH (referred to as Mg-Al LDH-BP) and Mg-Al LDO (referred to as Mg-Al LDO-BP) aqueous suspension, respectively. The SEM images of Mg-Al LDH-BP (Fig. 2a) and Mg-Al LDO-BP (Fig. 2b) illustrate that LDH and LDO are distributed on the fiber surface and have penetrated into the gaps within the paper fibers without damaging the microfiber morphology. Additionally, the element composition results demonstrate the main composition of C and O elements, accompanied by the distribution of Mg and Al on the fibers (Figs. 2c and d). To illustrate the penetration of Mg-Al LDH and LDO within the fibers, a simple test was conducted by sticking a piece of tape onto the treated paper surface and subsequently pulling it off. The results (Fig. S2a and b in Supporting information) reveal that even after being taped twice, residues of Mg-Al LDH/LDO remain evenly distributed on the paper fibers. This occurrence is probably attributed to the electrostatic interaction arising from the positively charged Mg-Al LDH/LDO nanoflakes during the dip-treating process onto the paper, facilitating their automatic adsorption onto the cellulose surface. This adsorption phenomenon is further supported by the zeta potential measurements of Mg-Al LDH and LDO nanoflakes (Fig. S3a in Supporting information). Moreover, the cross-section SEM images of the paper fibers (Fig. S2c in Supporting information) provide clear evidence that, following the deacidification treatment, the Mg-Al LDH/LDO materials effectively permeate through the entire layer of paper fibers, thus demonstrating the uniformity of the interaction between Mg-Al LDH/LDO and fibers as a whole, rather than being restricted merely to the surface. Additionally, these residues are not visible to the naked eye and have no impact on the appearance of paper. This is further supported by the results from CIE-Lab* system (Table S2 in Supporting information), which reveal only a negligible difference in discoloration (with little change in L, a*, b*) between BP before and after deacidification. Meanwhile, XRD analysis indicates that the crystallinity index (CrI) of BP, Mg-Al LDH-BP, and Mg-Al LDO-BP remained relatively stable at approximately 65%, 64%, and 62%, respectively, as calculated by the XRD peak height method (Fig. S3b in Supporting information) [29].

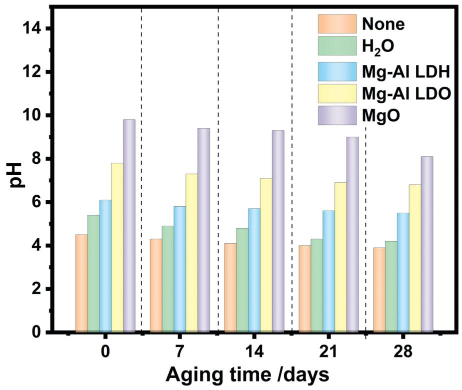

**Fig. 3.** pH values of BP and treated BP before and after accelerated aging for different times.

The BP acidifies during long-term natural storage and exhibits a low pH value of 4.5 (Fig. 3). Although washing with $H_2O$ can raise the pH value of BP ($H_2O$-BP) to 5.4, further deacidification is required to achieve a safe pH level for the paper. After deacidification with Mg-Al LDH and LDO, the pH values of treated BP are increased to 6.1 and 7.8, respectively. For evaluating the long-term deacidification performance of the protective materials, an artificial dry-heat accelerated aging process is commonly used. After 28 days of aging, the BP shows a decline in pH from 4.5 to 3.9, while $H_2O$-BP exhibits a decrease from 5.4 to 4.2. Remarkably, Mg-Al LDH-BP and Mg-Al LDO-BP exhibit the well-maintained pH values of 5.5 and 6.8 after aging for 28 days, respectively. The use of Mg-Al LDH and LDO effectively prevents the paper from undergoing significant pH decrease over time, providing long-lasting protection against acid-induced cellulose degradation. Quantitative analysis of the amount of alkaline reserve in Mg-Al LDH and Mg-Al LDO treated BP reveals values of 0.49 and 0.93 mmol $[OH^-]$/g, respectively, which are in accordance with the suggested value [13].

One of the noteworthy properties of hydrotalcite is its memory effect, in which LDO can be regenerated into LDH through rehydration. The resulting transformed LDH exhibits higher alkalinity than its original LDH, attributed to the partial presence of oxides [21]. In order to verify whether LDO transforms to the LDH crystalline phase through the memory effect while deacidifying in aqueous solution, and to further examine the crystalline phase of the reserved alkaline material on the paper, we intentionally increased the concentration of Mg-Al LDO aqueous suspension to 3 wt% (referred to as 3 wt% Mg-Al LDO-BP). The XRD pattern (Fig. 4a) clearly reveals the characteristic (003) diffraction peak of hexagonal Mg-Al LDH in 3 wt% Mg-Al LDO-BP, suggesting that the alkaline material retained in paper after LDO-deacidification is rehydrated LDH. Moreover, Mg-Al LDO material was centrifuged after deacidification and XRD tests were performed during its natural drying process to detect the transformation of the crystal phase of LDO. As shown in Fig. 4b, following a 15-min deacidification process, the wet residual LDO obtained by centrifugation retains the XRD crystalline phase of LDO, and after 6 h of natural drying, LDO gradually transforms

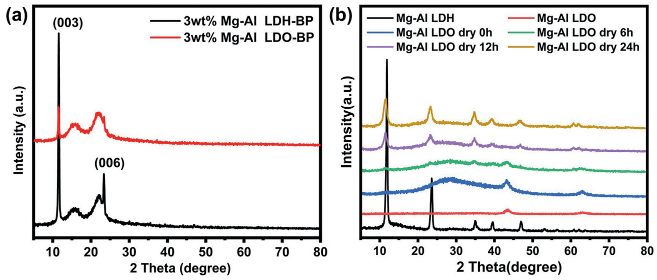

**Fig. 4.** (a) XRD patterns of Mg-Al LDH-BP and Mg-Al LDO-BP. (b) XRD patterns of Mg-Al LDO during the natural drying process after deacidification.

into rehydrate LDH and nearly completes this transformation by 12 h of drying. It also stabilizes as LDH phase at 24 h of drying. This indicates that Mg-Al LDO has converted to Mg-Al LDH during the natural drying process due to the memory effect, preventing the prolonged presence of highly alkaline materials that could result in alkaline damage, such as cellulose degradation and pigment discoloration. Hence, the LDH series of deacidifying materials have a wide range of applicability. In cases of heavily acidified paper, the higher alkalinity of LDO can be employed, and the rehydrated LDH with suitable alkalinity can be retained as the base. For slightly acidified paper, LDH can be directly employed as the deacidifying material. For example, Mg-Al LDH effectively raises the pH of paper from 5.5 to 6.3, 6.0 to 6.7 and 6.4 to 7.3, respectively, while Mg-Al LDO increases the pH of paper from 5.5 to 8.6 and from 6.0 to 8.8 (Fig. S4a in Supporting information). Moreover, Mg-Al LDO is more suitable for heavily acidified paper, such as raising the pH of BP from 4.3 to 7.7 and from 5.0 to 8.4, raising the pH of natural aged machine-made paper from 4.0 to 7.6 and from 5.1 to 8.5 (Fig. S4b in Supporting information). These results show the versatility and applicability of both Mg-Al LDH and Mg-Al LDO as effective deacidifying materials for a wide range of acidic conditions of paper, making them valuable tools in preserving and protecting paper-based relics. Additionally, there are reports of Mg-Al LDH dispersed in organic solvents for paper deacidification (raise pH of acidic paper from 4/4.1 to 4.6–7.83), which further demonstrates the wide solvent suitability of LDH-based materials [24,30,31].

It is well-known that paper made from natural plant fibers is susceptible to fire damage. The inherent nonflammability and thermal stability make LDH the excellent fire-resistant materials and ideal for shielding flammable paper objects [32]. As shown in Figs. 5$a_1$ and $a_3$, the BP and Mg-Al LDO-BP burns to ash within 20 and 50 s, respectively, and Mg-Al LDH-BP shows little change during a 50 s burning period (Fig. 5$a_2$). The thermal stability test results in Fig. S5 (Supporting information) further demonstrate that BP turns yellow at 200 °C and undergoes significant carbonization at 300 °C for 30 min. In contrast, Mg-Al LDH-BP shows the least color change when held at 300 °C for 30 min compared with those of BP and Mg-Al LDO-BP. This is attributed to the heat absorption during LDH decomposition, which contributes to the improved thermal stability of Mg-Al LDH-BP. Additionally, a stable and compact char residue prevents the diffusion of flammable gas and heat, resulting in effective flame retardancy, as supported by Figs. 5$b_1$–$b_3$ [33]. The lower total weight loss of 89.1% in Mg-Al LDH-BP than that of BP (95.4%, Fig. 5c) provide further confirmation of the excellent fire-resistance performance of Mg-Al LDH-protected paper [34].

Considering the possible color changes or losses that certain pigments or inks may experience in strongly alkaline solutions, sometimes even being irreversible, two commonly used pigments, Prussian blue ($Fe_4[Fe(CN)_6]_3$, denoted as PB) and lead tetroxide ($Pb_3O_4$, denoted as LT), were selected as the target objects for color fading tests. The results of the aging experiment were evaluated through color block contrast. As shown in Figs. 6a and b, the PB pigments mixed with MgO were found to be the most susceptible to fading, whereas the mixture of PB pigments with Mg-Al LDH/LDO exhibited only slight lightening, which can be attributed to the dilution effect of the white color of Mg-Al LDH/LDO. After deacidification with MgO, the pH value of BP increases from 4.5 to 9.8 (Fig. 3), and it remains at a pH of 9.3 even after 14 days of aging, potentially causing pigment discoloration due to the excessive pH level [35]. The corresponding CIE color coordinates (Table S3 in Supporting information) provide a more accurate confirmation of the above observation. In addition, the protective solutions of Mg-Al LDH and LDO were subsequently applied onto the paintings. As shown in Fig. 6c, no noticeable alterations, such as pigment blotching or color fading, were observed in the paintings following the application of the protective agents, in comparison to the original artworks. To investigate the potential impact of the Mg-Al LDH/LDO deacidifying materials on the writing performance of the paper, the water contact angle ($CA_{H_2O}$) measurements were performed (Fig. 6d). The contact angle of BP, Mg-Al LDH-BP and

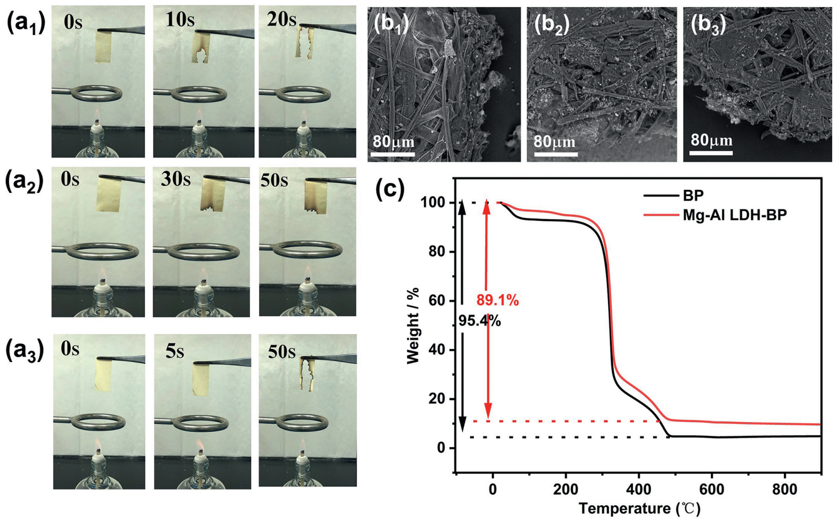

**Fig. 5.** Fire-resistance tests. Combustion processes and change of ($a_1$) BP, ($a_2$) Mg-Al LDH-BP and ($a_3$) Mg-Al LDO-BP. SEM images of ($b_1$) BP, ($b_2$) Mg-Al LDH-BP and ($b_3$) Mg-Al LDO-BP, after fire-resistance. (c) TGA of BP and Mg-Al LDH-BP.

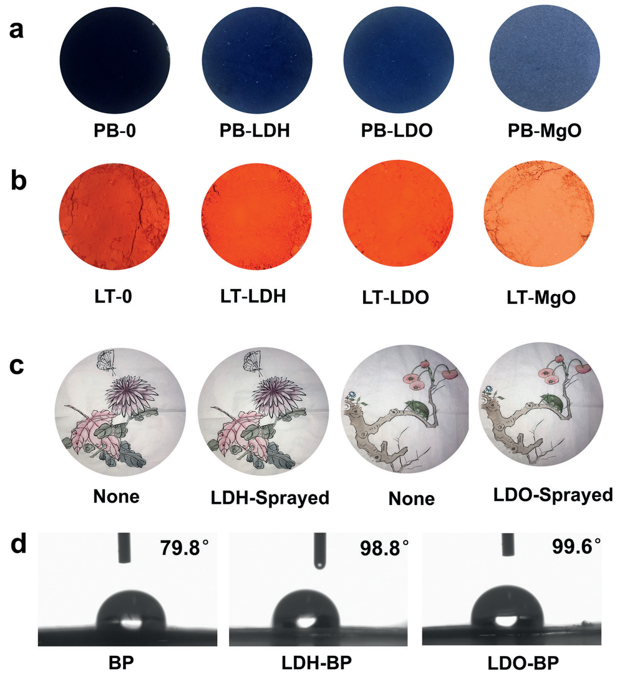

**Fig. 6.** The resistance experiments to alkaline materials of different pigments: photographs of (a) Prussian blue and (b) lead tetroxide, where pigments were mixed with different protective materials aqueous suspension (blank, Mg-Al LDH, Mg-Al LDO, MgO). (c) Images of the paintings before and after spaying Mg-Al LDH and LDO. (d) Contact angles of water droplets on the surface of BP, Mg-Al LDH-BP and Mg-Al LDO-BP.

Mg-Al LDO-BP is 79.8°, 98.8° and 99.6°, respectively, indicating that the wettability and writing performance of the paper remain unaffected by the treatment with a certain amount of Mg-Al LDH and Mg-Al LDO.

Paper fibers are susceptible to bacterial contamination both during usage and storage, which can subsequently result in the deterioration. It is crucial that deacidified paper possesses antimicrobial properties as well. To assess the antibacterial performance of Mg-Al LDH and LDO materials, we focused on investigating their inhibitory effects against representative bacteria, namely *Staphylococcus aureus* (denoted as SA) and *Escherichia coli* (denoted as EC). The petri dishes containing bacteria were incubated at 28 °C, 75% RH for 24 h, and several round pieces of paper (0.5 cm in diameter) used in the experiment were previously sterilized. The diameter of the inhibition zone for different bacteria, when exposed to various bacteriostatic agents (Fig. S6 in Supporting information), illustrates that cellulose paper itself lacks the ability to impede the growth of bacteria. However, it becomes evident that paper specimens treated with 1.0 wt% Mg-Al LDH (average inhibitory diameter of 1.08 and 1.0 cm for SA and EC, respectively) and 1.0 wt% Mg-Al LDO (average inhibitory diameter of 1.05 and 1.2 cm for SA and EC, respectively) exhibit a more potent antibacterial effect compared to that of untreated paper.

In conclusion, a facile and safe approach for the effective protection of acidified paper is proposed. This method employs layered double hydroxide (LDH)-based nanomaterials as deacidifying agents, characterized by their simplicity and safety in synthesis and cost-effectiveness. Mg-Al LDH and its calcined derivative, mixed metal oxide LDO, offer adjustable alkalinity, ensuring the appropriate level of deacidification protection for paper with varying levels of acidity. For instance, when dealing with severely acidified paper (*e.g.*, pH $\leq$ 5.5), LDO can serve as an effective deacidifying agent. During the aqueous phase deacidification process, LDO undergoes transformation into rehydrated LDH due to the memory effect, resulting in a mild and suitable alkaline retention within the paper. Additionally, it is worth noting that Mg-Al LDH/LDO demonstrate considerable flame retardancy, antibacterial capability and resistance to pigment discoloration, further enhancing their utility in multifunctional protection of acidified paper. This work opens up new possibilities for designing safe and efficient alkaline materials in paper-based relics protection and preservation.

## Declaration of competing interest

The authors declare that they have no known competing financial interests or personal relationships that could have appeared to influence the work reported in this paper.

## CRediT authorship contribution statement

**Sinong Wang:** Conceptualization, Data curation, Formal analysis, Funding acquisition, Resources, Supervision, Writing – original draft, Writing – review & editing. **Shanshan Jin:** Data curation, Formal analysis, Investigation, Visualization, Writing – original draft. **Xue Yang:** Validation, Formal analysis, Investigation. **Yanyan Huang:** Resources. **Peng Liu:** Resources. **Yi Tang:** Conceptualization, Project administration, Supervision. **Yuliang Yang:** Conceptualization, Resources, Supervision.

## Acknowledgments

We acknowledge financial support from the National Key R&D Program of China (No. 2022YFF0904200), Shanghai Rising-Star Program (No. 23QA1404100) and Key Laboratory of Pulp and Paper Science and Technology of Ministry of Education of China (No. KF201921).

## Supplementary materials

Supplementary material associated with this article can be found, in the online version, at doi:10.1016/j.cclet.2024.109890.

## References

[1] S.A. Buchanan, Pap. Conserv. 11 (1987) 69–72.
[2] J. Wouters, Science 322 (2008) 1196–1198.
[3] X. Zou, N. Gurnagul, T. Uesaka, et al., Polym. Degrad. Stab. 43 (1994) 393–402.
[4] P. Calvini, A. Gorassini, A.L. Merlani, Cellulose 15 (2008) 193–203.
[5] M.A. Mellmer, C. Sener, J.M.R. Gallo, et al., Angew. Chem. Int. Ed. 53 (2014) 11872–11875.
[6] S. Zervos, I. Alexopoulou, Cellulose 22 (2015) 2859–2897.
[7] A.L. Dupont, B. Lavédrine, H. Cheradame, Polym. Degrad. Stab. 95 (2010) 2300–2308.
[8] R. Giorgi, M. Baglioni, D. Berti, et al., Acc. Chem. Res. 43 (2010) 695–704.
[9] S.S. Jin, S.N. Wang, Acta Chim. Sin. 81 (2023) 309–318.
[10] F. Sundholm, M. Tahvanainen, Restaurator 25 (2004) 15–25.
[11] B. He, Q. Lin, M. Chang, et al., Carbohydr. Polym. 209 (2019) 250–257.
[12] Y. Fang, X. Liu, H. Zheng, et al., Carbohydr. Polym. 235 (2020) 115782.
[13] K. Ahn, T. Rosenau, A. Potthast, Cellulose 20 (2013) 1989–2001.
[14] K. Jana, Restaurator 18 (1979) 163–176.
[15] Q. Zhou, Y. Liu, L. Wang, et al., Chem. Eng. J. 469 (2023) 143962.
[16] Y. Gao, Z. Zhang, J. Wu, et al., J. Mater. Chem. A 1 (2013) 12782–12790.
[17] S. Dutta, A. Indra, Y. Feng, et al., Appl. Mater. Interfaces 9 (2017) 33766–33774.
[18] Q. Wang, J.P. Undrell, Y. Gao, et al., Macromolecules 46 (2013) 6145–6150.
[19] Z. Gu, S. Yan, S. Cheong, et al., J. Colloid Interface Sci. 512 (2018) 404–410.
[20] R. Pourfaraj, S.J. Fatemi, S.Y. Kazemi, et al., J. Colloid Interface Sci. 508 (2017) 65–74.
[21] D. Kwon, J.Y. Kang, S. An, et al., Energy Chem. 46 (2020) 229–236.
[22] S. Wang, X. Yang, Y.H. Li, et al., J. Colloid Interface Sci. 607 (2022) 992–1004.
[23] S.Q. Lei, S.N. Wang, B.X. Gao, et al., J. Colloid Interface Sci. 577 (2020) 181–190.
[24] J. Jurišová1, V. Danielik1, S. Malečková, et al., Chem. Pap. 78 (2024) 1719–1730.
[25] L. Wang, H. Xing, S. Zhang, et al., Biomaterials 34 (2013) 3390–3401.
[26] Y. Wen, S. Yu, W. Jian, et al., Chem. Eng. J. 307 (2017) 476–486.
[27] M.X. Zhu, Y.P. Li, M. Xie, et al., J. Hazard. Mater. 120 (2005) 163–171.
[28] H. Zaghouane-Boudiaf, M. Boutahala, L. Arab, Chem. Eng. J. 187 (2012) 142–149.
[29] S. Nomura, Y. Kugo, T. Erata, Cellulose 27 (2020) 3553–3563.

[30] M. Králik, S. Katuščák, P. Fellner, et al., SSRN Electron. J. (2023), doi:10.2139/ssrn.4330690.
[31] E. Guzikiewiczová, S. Malečková, J. Jurišová, et al., Res. Sq. (2023), doi:10.21203/rs.3.rs-3061945/v1.
[32] P. Ding, B. Kang, J. Zhang, et al., J. Colloid Interface Sci. 440 (2015) 46–52.
[33] S. Xu, M. Zhang, S.Y. Li, et al., Appl. Clay Sci. 191 (2020) 105600.
[34] F.F. Chen, Y.J. Zhu, Z.C. Xiong, T.W. Sun, Y.Q. Shen, ACS Appl. Mater. Interfaces 8 (2016) 34715–34724.
[35] H. Zhang, C. Zhang, Z. Ye, et al., Microporous Mesoporous Mater. 293 (2020) 109786.